Contemporary Mathematics
https://ojs.wiserpub.com/index.php/CM/

Research Article

A Multi-Dimensional and Multi-Level Based Collaborative Evaluation of Carbon Reduction in the Power Sector

Jiang Bian[1], Yang Wang[2], Tianchun Xiang[2*]

[1] State Grid Tianjin Electric Power Research Institute, Tianjin, 300384, China
[2] State Grid Tianjin Electric Power Company, Tianjin, 300010, China
E-mail: tianchun.xiang@tj.sgcc.com.cn

Received: 6 May 2025; **Revised:** 28 September 2025; **Accepted:** 10 October 2025

Abstract: Achieving deep carbon reduction in the power sector is central to China's green energy transition. This study develops a novel multidimensional and multi-level collaborative evaluation framework designed specifically to assess carbon reduction pathways in electricity systems. Methodologically, we begin by forecasting power demand and the evolution of the generation structure—including thermal, wind, hydro, and photovoltaic sources—based on multi-source power big data, which provides a high-resolution foundation for model parameterisation and calibration. An improved Analytic Hierarchy Process-Entropy Weight Method (AHP-EWM) integrated with a Particle Swarm Optimization (PSO) algorithm is proposed, where the availability of big data facilitates a more robust training process for the PSO, leading to scientifically robust weights for these indices. The model subsequently evaluates the synergistic efficiency of carbon reduction strategies, incorporating constraints on both carbon and air pollutant emissions to quantify co-benefits. Applied to a representative Chinese province from 2030 to 2050, the model demonstrates that under the AHP-EWM-PSO optimized scenario, carbon reduction efficiency is maximized. By 2050, carbon dioxide emissions are projected to decrease significantly, accompanied by substantial reductions in air pollutants, confirming the strong synergistic outcomes of the proposed pathway. The coupling degree of synergy approaches 1, indicating optimal alignment between carbon mitigation and auxiliary environmental benefits. This study provides a scientifically-grounded and practical tool for formulating and monitoring carbon reduction strategies, supporting policy-making aimed at accelerating the transition to a high-renewable power system with significant environmental co-benefits.

***Keywords*:** carbon reduction, collaborative evaluation, power big data, low-carbon transition

MSC: 90C90, 91B76, 93A30

1. Introduction

With the development of the global economy, carbon emissions have become a critical issue significantly impacting global climate change. As a country with prominent "high-carbon" characteristics in its energy, economic, and social development, China faces substantial challenges in achieving its "Dual Carbon" goals (carbon peak and carbon neutrality). The power sector, being a major carbon emitter, plays a pivotal role in this transition. Fortunately, the low-carbon transformation of the power industry—mainly through reducing coal consumption and increasing the share of renewable

DOI: https://doi.org/10.37256/cm.7220267182

energy—not only directly mitigates carbon emissions but also concurrently leads to significant reductions in atmospheric pollutants. This synergistic effect provides a valuable co-benefit that enhances the overall environmental and health outcomes of carbon mitigation policies [1].

Against this backdrop, it is essential to establish a scientifically robust framework for evaluating the effectiveness and co-benefits of carbon reduction pathways. Existing studies have laid a preliminary foundation for integrated environmental governance. For instance, Chen et al. [2] employed a comprehensive evaluation model, a coupling coordination degree model, and a Panel Vector Autoregression (PVAR) model to examine the coupling and interactive effects between synergistic carbon reduction efficiency and economic quality. Their findings revealed a mutually reinforcing relationship between these two dimensions. Wang et al. [3] adopted the hierarchical analysis (Analytic Hierarchy Process (AHP)) method to determine the weights of various indicators and the linear weighting function method to obtain the coordination degree of urban pollution reduction and carbon reduction, forming an evaluation index system of urban pollution reduction and carbon reduction coordination degree. Wang et al. [4] evaluated and analyzed the synergistic emission reduction effects of SO_2, NO_x, and carbon dioxide through the coordinate system analysis method of synergistic control effects and the cross-elasticity analysis method of pollutant emission reduction. Using the improved Tapio decoupling principle and Probit model, Liu et al. [5] studied the synergies between Pollution Reduction (PR) and Carbon Reduction (CR), providing valuable insights for formulating urban sustainable development policies. Zha [6] is based on the Non-radial Directional distance Function (NDDF) model to measure the efficiency of urban carbon reduction collaborative governance. Subsequently, Arc Geographic Information System (ArcGIS) and spatial autocorrelation analysis were employed to examine its spatial distribution characteristics, while a spatial econometric model was applied to investigate the underlying driving factors. Zhu et al. [7] and Xiang et al. [8] further highlighted the importance of the power sector and explored pathway optimizations under varying electricity demand scenarios.

However, most existing research remains qualitative or theoretical in nature, with limited multi-dimensional quantitative evaluation on the synergy level and effectiveness of carbon reduction. Commonly adopted methods also often suffer from low accuracy, high computational complexity, and limited practical applicability. Although evaluation methods such as AHP help structure decision-making, they tend to rely heavily on subjective judgment. While the entropy weight method can introduce objectivity, it still lacks a feedback mechanism for dynamically optimizing indicator weights based on evaluation outcomes [9, 10].

To address these limitations, this study constructs a multi-dimensional and multi-level collaborative evaluation system by leveraging the power of big data. The volume, variety, and velocity of big data enable a more granular and dynamic parameterisation of the model, which is designed specifically to assess carbon reduction performance and its synergistic benefits. An improved algorithm combining AHP, the Entropy Weight Method (EWM), and Particle Swarm Optimization (PSO) is proposed to optimize the comprehensive weights of evaluation indicators. On this basis, the carbon reduction and synergy benefits are calculated. The coupling degree between these metrics serves as tangible evidence validating the effectiveness and multiple benefits of carbon reduction pathways. Critically, the PSO algorithm's search for optimal weights is significantly enhanced by the rich, real-world dataset, which provides a comprehensive landscape for the fitness function to evaluate solutions against. This approach offers a more scientific, dynamic, and practical tool for supporting the power sector's transition toward a sustainable and low-carbon future [11–18].

2. Synergies in carbon reduction through power sector transition

This study focuses on the low-carbon transformation of the power sector. The corresponding evaluation indices, derived from power demand forecasts and structural evolution, are designed to assess the effectiveness of decarbonization pathways. The utilisation of big data is instrumental throughout this process, not only for initial forecasting but also for the subsequent optimisation of the evaluation model. The high-dimensional and temporal nature of the data allows for a more precise identification of key influencing factors and their interrelationships, which directly informs and improves the weight allocation process in the optimization model. It is noteworthy that these pathways also lead to significant co-

reductions in air pollutants—a synergistic benefit reinforcing the environmental advantages of transitioning to a cleaner energy mix.

Table 1 summarizes key parameters relevant to carbon emission reduction and associated pollution mitigation within the power industry. Historical and projected data—including installed capacity, capacity factors, and generation hours for various power sources—were collected from official reports published by the China Electricity Council and operational datasets from provincial power grids. Emission factors for CO_2 and SO_2 from thermal power generation were referenced from the Intergovernmental Panel on Climate Change (IPCC) Emission Factor Database, supplemented with real-world monitoring data from Chinese power plants. Additional energy consumption data across major industrial and transportation sectors were obtained from the China Statistical Yearbook and provincial statistical yearbooks.

Table 1. Parameters for carbon emission reduction in the power industry

Power supply type	Parameter	Value
Wind power	Rated wind speed	12-15 m/s
	Cut-in wind speed	3-4 m/s
	Cut-out wind speed	22-25 m/s
Hydropower	Power generation efficiency	0.85-0.92
	Power generation head	50-100 m
	Power generation flow	500-1,000 m^3/s
Photovoltaic	Standard light intensity	1,000 W/m^2
	Power temperature coefficient	-0.004 °C
Thermal power	Climbing speed constraint	Cold state: 1-3% P_{max}/min
		Hot state: 3-5% P_{max}/min
	Emission coefficient	CO_2: 0.85 kg/kWh
		SO_2: 0.8 kg/kWh

2.1 *Power demand forecast*

Reasonable allocation of power resources according to the forecast results of power generation can ensure the balance of supply and demand in the power system. This can reduce the situation of oversupply or insufficient power supply, reduce energy waste, and improve energy utilization efficiency [19].

$$E = \sum_i C_i \times h_i \tag{1}$$

where, E is the power generation, kW·h; i indicates the type of power supply. C is the installed capacity of the power supply, kW; h is the power generation utilization hours of each power source.

2.2 *Power output characteristics*

2.2.1 *Wind power output*

The power generation capacity and power generation of wind farms strongly depend on wind energy, and the wind power output is mainly restricted by wind speed, rated wind speed, and other parameters [20]. The wind power output model is shown as follows:

$$P_{W,t}=\begin{cases}0 & 0\leqslant V_t\leqslant V_I\\ \dfrac{V_t^3-V_I^3}{V_r^3-V_I^3}P_{W,r} & V_I<V_t\leqslant V_r\\ P_{W,r} & V_R<V_t\leqslant V_O\\ 0 & V_O<V_t\end{cases} \tag{2}$$

where: $P_{W,r}$ is the rated output of wind power; $P_{W,t}$ is the wind power output during the period of t; V_t is the wind speed during the t period; V_I is the cut-in wind speed of the fan; V_r is the rated wind speed of the fan; V_O is the cut-out wind speed of the fan.

Based on the predicted wind power output, the following relationships [21] are met:

$$0\leqslant P_{W,t}^{p}\leqslant P_{W,t}^{f} \tag{3}$$

where: $P_{W,t}^{p}$ and $P_{W,t}^{f}$ are respectively the planned and predicted wind power output at time t. The prediction error of wind power output follows the Laplacian normal mixed distribution.

The actual output of wind power [21] is:

$$P_{W,t}=P_{W,t}^{f}+\Delta P_{W,t}^{f} \tag{4}$$

where: $P_{W,t}$ and $P_{W,t}^{f}$ is the actual output and predicted error of wind power at time t.

2.2.2 *Hydropower output*

The output of hydropower units primarily depends on three factors: efficiency (η), water flow rate (Q), head (H), and water-electricity conversion coefficient 9.81. The basic formula of hydropower output [22] is:

$$P_h^t=9.81\eta_h Q_h^t H_h^t \tag{5}$$

2.2.3 *Photovoltaic power generation output*

Photovoltaic generation uses the solar photovoltaic module's photoelectric effect to produce electricity; its output is mainly affected by light intensity, temperature, and other factors. The photovoltaic output model [20] is as follows:

$$P_{PV,t}=P_{PV,r}\frac{L_t}{L_r}\left[1-\varepsilon\left(T_t-T_r\right)\right] \tag{6}$$

where, is $P_{PV,t}$ the photovoltaic output of the t period; $P_{PV,t}$ is the Photovoltaic output under standard conditions; T_t is the temperature during the t period; L_t is the ground light intensity of the current period; L_r is the light intensity under standard

conditions; T_t is the temperature under standard conditions; ε is the power temperature coefficient. The forecasting errors of Photovoltaic (PV) output conform to a normal distribution $N\left(0,\ {\sigma_{PV,t}}^2\right)$.

The actual output of photovoltaic power generation [21] is:

$$P_{PV,t} = P^f_{PV,t} + \Delta P^f_{PV,t} \tag{7}$$

where: $P_{PV,t}$ and $\Delta P^f_{PV,t}$ is the actual output and predicted error of wind power at time t.

2.2.4 *Thermal power output*

For thermal power units, to ensure the stable operation and economy of the unit, as well as its technical reasons or fuel reasons, are blocked, its maximum output is the installed capacity of the unit minus the capacity of the blocked part, which will lead to a reduction of the regulatory capacity of the thermal power unit. The output power of the controllable power supply has upper and lower limits, and the total power generation of some units is limited for some time [20].

Output limited characteristics:

$$P_{i,\min} \le P_i \le P_{i,\max} \tag{8}$$

Power generation limited characteristics:

$$E_{\min} \le E = \sum_{i=n_1}^{n_2} P_i \le E_{\max} \tag{9}$$

Climbing speed constraint characteristics:

$$\Delta P_{\max} \le P_{i+1} - P_i \le \Delta P_{\max}. \tag{10}$$

2.3 *Limits on total carbon emissions and carbon-driven pollution reduction*

Achieving the "Dual Carbon" goals necessitates a fundamental transition toward low-carbon development in the power sector, which is a major contributor to CO_2 emissions due to its historical reliance on fossil fuels. This subsection establishes a constraint on total carbon emissions to guide and evaluate the sector's decarbonization pathway. The emission limit is derived based on power demand forecasts and accounts for the pivotal role of the power industry in enabling carbon reduction across key sectors, including energy, industry, transportation, construction, and the economy.

The total carbon emission limit is calculated by the following formula [8]:

$$\sum_{i=1}^{I} f_{E_{i,t,c}} E_{i,t} + \sum_{j=1}^{J} f_{F_{j,t,c}} F_{j,t} + \sum_{m=1}^{M} f_{H_{m,t,c}} H_{m,t} + \sum_{n=1}^{N} f_{T_{n,t,c}} T_{n,t} \le CM \tag{11}$$

where, CM is the upper limit of total carbon emission control, t.

It is important to note that the transition to a low-carbon power structure—characterized by increasing penetration of renewables and reduced coal-based generation—inherently leads to significant co-reductions in air pollutants. Thus, while the primary focus remains on carbon mitigation, the associated decline in atmospheric pollutants such as SO_2, NO_x,

and $PM_{2.5}$ serves as a critical synergistic outcome. The following expression estimates the concurrent reduction in air pollutants resulting from the decarbonization of the power and related sectors:

$$\sum_{i=1}^{I} f_{E_{i,t,p}} E_{i,t} + \sum_{j=1}^{J} f_{F_{j,t,p}} F_{j,t} + \sum_{m=1}^{M} f_{H_{m,t,p}} H_{m,t} + \sum_{n=1}^{N} f_{T_{n,t,p}} T_{n,t} \leq PM \tag{12}$$

where, i represents the major industries of carbon emission, including steel, chemical, building materials, and other coal industries; $E_{i,t}$ represents the energy consumption of various sectors, t; j denotes power generation mode, including thermal power, nuclear power, hydropower, wind power and solar power, $F_{j,t}$ denotes power generation, kW·h; m represents the heating mode, including coal-fired heating and non-coal-fired supply, $H_{m,t}$ represents the heating capacity, $109J$; n represents the mode of transportation, including gasoline vehicles and new energy vehicles, $T_{n,t}$ represents the energy consumption of transportation, gasoline vehicles are L, electric vehicles are kW·h; p indicates the type of pollutant; $f_{E_{i,j,p}}$, $f_{F_{j,t,p}}$, $f_{H_{j,t,p}}$, and $f_{T_{n,t,p}}$ are emission coefficient per unit of industrial production, emission coefficient per unit of power generation, emission coefficient per unit of heating and emission coefficient per unit of traffic. PM is the upper limit of total air pollutants (e.g., SO, NO_x, $PM_{2.5}$) control, t. The specific data sources are as follows: Industrial Emission: China Statistical Yearbook; Power Sector: China Electricity Council (CEC) Reports, IPCC Emission Factor Database and Power Plant Monitoring Data; Heating Sector: Provincial Energy Bureaus and MEE Urban Emission Inventories; Transport Sector: Ministry of Transport Statistics.

3. Optimization model

3.1 *Index system*

Based on existing research on low-carbon transition and carbon reduction evaluation systems, this study constructs a comprehensive evaluation index model centred on the decarbonization of the power sector. The model is structured into three hierarchical levels: the target layer (A), the criterion layer (B), and the indicator layer (C).

The criterion layer encompasses critical dimensions that influence the effectiveness of carbon emission reduction driven by the power sector's structural transformation. The indicator layer further specifies measurable strategies and factors corresponding to each criterion, which collectively facilitate and reflect progress in carbon mitigation. The target layer synthesizes the multi-dimensional evaluation results, delivering a holistic assessment of the performance and synergistic benefits of the low-carbon transition—including but not limited to associated reductions in air pollutants. This integrated framework supports the systematic quantification and optimization of pathways toward a sustainable, low-carbon power system [23–26].

3.2 *Weight optimization model*

3.2.1 *Subjective weight*

The scoring matrix is generated by using expert scoring [27]. Expert rating result d_{ij} represents experts' ratings on the relative importance of different evaluation dimensions. Experts rank the importance of each indicator, score according to national emission standards and historical experience, give judgment matrix factors, and construct judgment matrix D [28].

Each judgment matrix D:

$$D = \begin{bmatrix} d_{11}, d_{12}, \ldots, d_{1n} \\ d_{21}, d_{22}, \ldots, d_{2n} \\ d_{n1}, d_{n2}, \ldots, d_{nn} \end{bmatrix} \tag{13}$$

where, the order n is the number of indicators that need to be compared in each dimension.

The judgment matrix D is satisfied:

$$d_{ij} = 1/d_{ji}, \quad \forall i, j, \quad d_{ij} > 0 \tag{14}$$

The matrix transformation process is carried out on the judgment matrix D. After each column of the judgment matrix D is normalized, each factor in the matrix is μ_{ij}, as shown below:

$$\beta_i = \sum_{j=1}^{n} \mu_{ij}, \quad i, j = 1, 2, \ldots, n \tag{15}$$

The judgment matrix is further added on A row basis to produce an $n \times 1$ column vector where each term is defined as β_i, as shown below:

$$\beta_i = \sum_{j=1}^{n} \mu_{ij}, \quad i, j = 1, 2, \ldots, n \tag{16}$$

Normalize the column vector β_i to get a new $n \times 1$ column vector, in which each term is defined as ω_i, as follows:

$$\omega_i = \beta_i / \sum_{i=1}^{n} \beta_i, \quad i = 1, 2, \ldots, n \tag{17}$$

where, ω_i is the subjective weight, and its relative weight vector is as follows: $W_i = (\omega_1, \omega_2, \ldots, \omega_n)^T$.

3.2.2 *Objective weight*

The reference information matrix is generated using the objective reference information a_{ij} for each evaluation dimension. For example, the above objective reference information is normalized to obtain the standardized information matrix X.

Objective reference information a_{ij} is used to characterize the objective factors that impact the evaluation results, such as the degree of improvement (reduction) in actual water environmental quality, the degree of improvement (reduction) in actual air quality, and the degree of improvement (decrease) in new energy utilization [29].

Element x_{ij} in the standardized information matrix X is shown as follows:

$$x_{ij} = \begin{cases} \dfrac{a_{ij} - a_{\min}}{a_{\max} - a_{\min}}, & a_{ij} \text{ is a positive indicator} \\ \dfrac{a_{\max} - a_{ij}}{a_{\max} - a_{\min}}, & a_{ij} \text{ is a negative indicator} \end{cases} \tag{18}$$

where, x_{ij} is an element in the standardized information matrix X, $a_{\max}$ is the maximum value of objective factors that impact the evaluation results, and amin is the minimum value of objective factors that impact the evaluation results.

The standardized information matrix X is converted into the information gravity matrix P. The single element value p_{ij} in the information gravity matrix P is used for characterization: The ratio of the unit information x_{ij} represented by a single evaluation dimension to the total information represented by multiple evaluation dimensions. Calculate the value p_{ij} of a single element in the information gravity matrix P, as follows:

$$P_{ij} = \frac{x_{ij}}{\sum_{i=1}^{n} x_{ij}} \tag{19}$$

The information entropy e_{ij} of each element in the information gravity matrix P is calculated. The information entropy e_{ij} represents the uncertainty degree of the objective reference information of each evaluation dimension.

Calculate the information entropy e_{ij}, as follows:

$$e_{ij} = -\frac{1}{\ln(n)} \sum_{i=1}^{n} P_{ij} \ln(P_{ij}) \tag{20}$$

Based on the information entropy of each element in the information gravity matrix, the objective weights ω_j of multiple evaluation dimensions are generated, as follows:

$$\omega_j = \frac{\sum_{j=1}^{n} e_{ij} + 2 - 3e_{ij}}{\sum_{i=1}^{n} \left(\sum_{j=1}^{n} e_{ij} + 2 - 3e_{ij} \right)}. \tag{21}$$

3.2.3 *Subjective and objective comprehensive weight*

Combine the subjective weight ω_i and objective weight ω_j to give the comprehensive weight $\omega_{i,j}$, as shown in the formula:

$$\omega_{ij} = \frac{\sqrt{\omega_i \omega_j}}{\sum_{i,j=1}^{n} \sqrt{\omega_i \omega_j}, \ i = 1, 2, \ldots, n} \tag{22}$$

3.2.4 *PSO optimization comprehensive weight*

The PSO algorithm formulates solutions to optimization problems by employing a population of particles that navigate a finite-dimensional space. Mathematically, each particle within this population is described by a pair of vectors denoting its instantaneous position and velocity. All particles cooperate to find a better position through their optimal value and the optimal value of the particle swarm. Each particle uses the fitness function to evaluate its position. All particle swarm particles are searched based on the position of the current optimal particle in the solution space [30].

Particle position update method, such as the formula:

$$x_{id}^{k+1} = x_{id}^{k} + v_{id}^{k+1} \tag{23}$$

The updating method of particle velocity is as follows:

$$v_{id}^{k+1} = wv_{id}^{k} + c_1 r_1 \left(p_{id} - x_{id}^{k} \right) + c_2 r_2 \left(p_{gbest} - x_{id}^{k} \right) \tag{24}$$

where, v_{id}^{k} represents the velocity of particle i in the d_{th} dimension at k iterations; x_{id}^{k} represents the position of particle i in the d_{th} dimension at the k iteration; w is the inertia weight; p_{id} is the optimal position of particle i; p_{gbest} is the optimal location of particle population. c_1 and c_2 are acceleration factors, usually 2; r is the random number between [0, 1].

To enhance the global optimization ability of the initial particle swarm and facilitate its escape from local optimal solutions, a dynamic inertia weight ω is introduced to aid individual particles in overcoming local optima. After improvement, the position x formula and dynamic inertia weight ω formula are updated as follows:

$$x_{id}^{k+1} = \begin{cases} N\left(\dfrac{p_{id} + p_{gbest}}{2}, \left| p_{id} - p_{gbest} \right| \right), & r < 0.5 \\ p_{id}, & r \geq 0.5 \end{cases}$$

$$\omega = \begin{cases} \omega_{\min} - \dfrac{(\omega_{\max} - \omega_{\min})}{F_{avg} - F_{\min}}, & F \leq F_{avg} \\ \omega_{\max}, & F \geq F_{avg} \end{cases} \tag{25}$$

where F is the current objective function of the particle.

Table 2 shows the comparative analysis of optimization algorithms.

Table 2. Comparative analysis of optimization algorithms

Method	Advantages	Disadvantages
Particle Swarm Optimization [30]	Global search with local refinement; few parameters; efficient for large scale power data.	Randomness affects reproducibility; sensitive to initial swarm position.
Genetic Algorithm [31]	Robust in complex landscapes; handles discrete variables.	High computational cost per iteration; requires tuning of crossover/mutation rates.
Simulated Annealing [32]	Guarantees global optimum asymptotically; simple implementation.	Slow convergence; sensitive to cooling schedule.
Ant Colony Optimization [33]	Effective for path optimization; self-adaptive.	Memory-intensive; struggles with continuous variables.

4. Solution of the low-carbon transition optimization model

4.1 *Carbon reduction synergy level*

A linear weighting function method is employed to comprehensively evaluate the synergy level of carbon emission reduction resulting from the low-carbon transition of the power sector [27]:

$$T = \omega_1 \sum_{j=1}^{7} \omega_{1j} S_{1j} + \omega_2 \sum_{j=1}^{8} \omega_{2j} S_{2j} + \ldots + \omega_9 \sum_{j=1}^{2} \omega_{9j} S_{9j} \tag{26}$$

where, T is the evaluation score; S is the score of each factor; ω_i and ω_{ij} are the comprehensive weights of the criterion and index layers.

4.2 *Cooperation degree index of carbon reduction*

Based on the total carbon emission constraint, the cooperation degree index of carbon reduction is calculated to quantify the alignment between actual emission reductions and the decarbonization targets [9]:

$$C = \frac{\Delta PM}{PM} / \frac{\Delta CM}{CM} \tag{27}$$

4.3 *Synergistic coupling degree of carbon reduction*

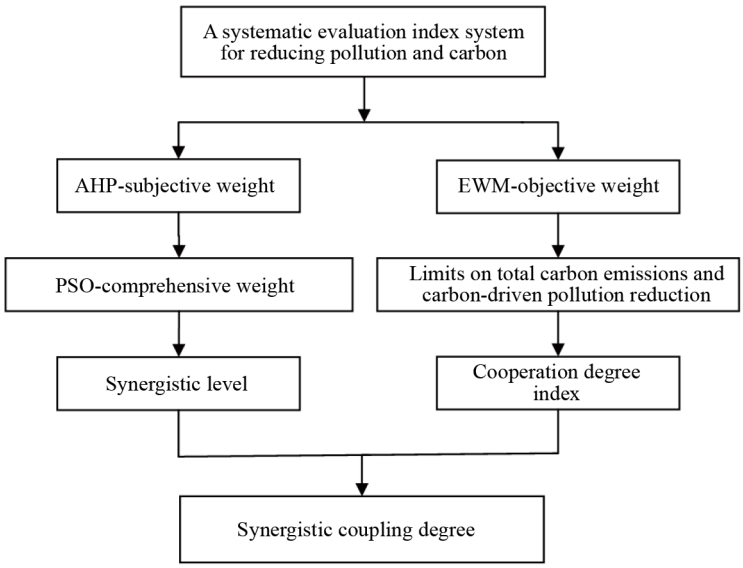

Figure 1. Method for generating evaluation results of carbon reduction under the low-carbon transition of the power sector

The synergistic coupling degree evaluates the systemic coordination between the achievement of carbon reduction targets and the overall transition efficiency of the power sector [31]:

$$TC = \alpha T + \beta C \tag{28}$$

where, TC denotes the comprehensive coupling coefficient reflecting the coordination between carbon reduction performance and pathway effectiveness, T represents the synergy level of carbon emission reduction, and C indicates the cooperation degree index related to emission constraint compliance [34]. The process is shown in Figure 1.

5. Result analysis

5.1 *Scenario setting*

In one province, for example, the current power industry mainly relies on fossil fuels such as coal and natural gas to generate electricity. With the adjustment of the power structure and optimization of power supply layout, inefficient coal-fired power generation has been phased out, and new energy sources have been vigorously developed.

Figure 2 shows the power generation structure of different types of power supplies. From 2030 to 2050, the share of thermal power will decline from 72% to 20%, while the share of wind power and photovoltaic power will continue to rise, and the share of hydropower will change steadily.

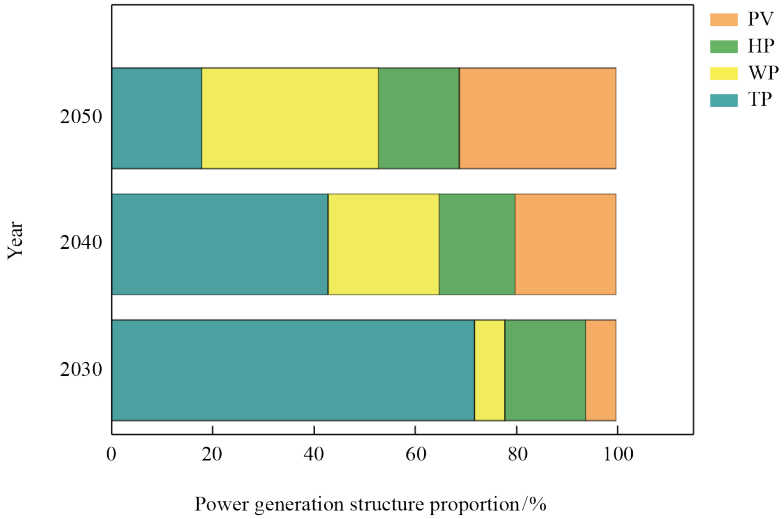

Figure 2. Different types of power generation

By promoting economic efficiency and simultaneously constraining high-energy-consuming industries, carbon emissions, and the fulfilment of carbon reduction goals, the power system's low-carbon transition delivers collaborative pollution reduction benefits.

5.2 *Future power forecast*

To develop a reasonably low-carbon electricity development path, it is necessary to predict future electricity demand reasonably. Electricity demand is closely related to social and economic development, scientific and technological progress, and improvements in energy efficiency, among other factors. Future electricity demand should be estimated based on past trends and reasonable assumptions.

This paper forecasts the electricity demand from 2030 to 2050, as shown in Figure 3. The electricity consumption in 2050 is 1.2×10^4 kW·h, primarily due to the elimination of a large number of thermal power generation units and the increase in new energy power generation, which could stimulate further electricity consumption.

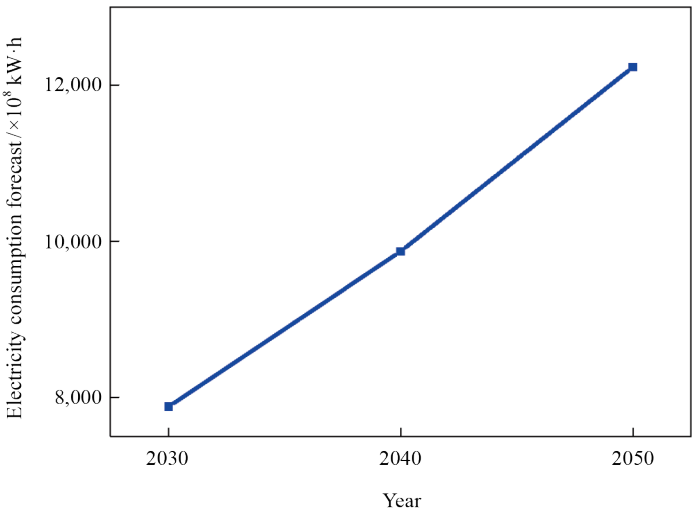

Figure 3. Power generation forecast

The forecast of power generation structure and power demand determines the evaluation indexes for carbon reduction performance, as detailed in the Appendix.

5.3 *Solving the carbon reduction evaluation model*

5.3.1 *Subjective weight*

A number of experts evaluated the relative importance of indicators at each layer within the assessment system for the low-carbon transition of the power sector, scoring each indicator based on its significance. Taking the criterion layer as an example, the index score of the criterion layer under the AHP is shown in Figure 4.

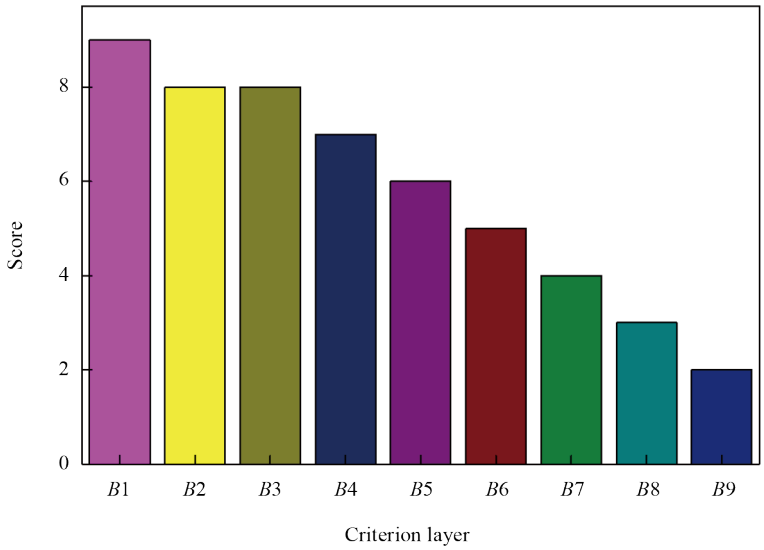

Figure 4. Index scores at the criterion level under AHP

According to the constructed index system and importance degree, the judgment matrix factors of each part are given, and the judgment matrix is built.

After further processing the judgment matrix D, the subjective weights of each index are obtained $W_{A-B}^{S} = (0.257, 0.171, 0.180, 0.145, 0.105, 0.073, 0.040, 0.029, 0)^{T}$.

$$D_{A-B} = \begin{Bmatrix} 1 & 2 & 2 & 3 & 4 & 5 & 6 & 6 & 8 \\ 1/2 & 1 & 1 & 2 & 3 & 3 & 4 & 6 & 8 \\ 1/2 & 1 & 1 & 2 & 4 & 4 & 5 & 5 & 7 \\ 1/3 & 1/2 & 1/2 & 1 & 3 & 3 & 5 & 6 & 8 \\ 1/4 & 1/3 & 1/4 & 1/3 & 1 & 3 & 5 & 5 & 7 \\ 1/5 & 1/3 & 1/4 & 1/3 & 1/3 & 1 & 4 & 4 & 6 \\ 1/6 & 1/4 & 1/5 & 1/5 & 1/5 & 1/4 & 1 & 3 & 5 \\ 1/6 & 1/6 & 1/5 & 1/6 & 1/5 & 1/4 & 1/3 & 1 & 6 \\ 1/8 & 1/8 & 1/7 & 1/8 & 1/7 & 1/6 & 1/5 & 1/6 & 1 \end{Bmatrix}$$

5.3.2 *Objective weight*

Using the objectivity of entropy weight method, the objective weight of the index is calculated. Through 4 experts, the scores of each evaluation index are obtained, and the objective weight is determined. Figure 5 shows the criterion-level index scores under the Entropy Weight Method (EWM).

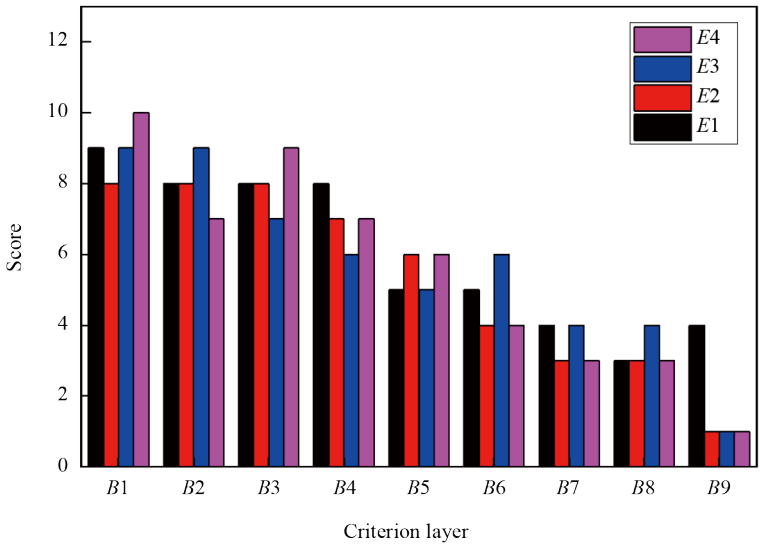

Figure 5. Index scores at the criterion level under EWM

After further processing, the objective weights of each criterion layer index are obtained, $W_{A-B}^{O} = (0.118, 0.118, 0.118, 0.118, 0.119, 0.119, 0.023, 0.120, 0.147)^{T}$.

5.3.3 *Empowering subjective and objective sets*

The comprehensive weights of indicators are calculated by combining the AHP and the improved entropy weight method [35, 36]. The comprehensive subjective and objective weights of the criterion layer are shown in Table 3. Taking the energy and industrial fields as examples, the comprehensive subjective and objective weights of each indicator layer are shown in Table 4.

Table 3. Comprehensive subjective and objective weights of criteria layer

Case	Comprehensive weight		
Index	B_1	B_2	B_3
Weight	0.196	0.160	0.164
Index	B_4	B_5	B_6
Weight	0.148	0.126	0.105
Index	B_7	B_8	B_9
Weight	0.034	0.066	0

Table 4. Comprehensive subjective and objective weights of each index layer

Case	Comprehensive weight		
Index	C_{11}	C_{12}	C_{13}
Weight	0.073	0.035	0
Index	C_{21}	C_{22}	C_{23}
Weight	0.076	0.028	0

5.3.4 *PSO method to optimize the comprehensive weight*

Because the determination of comprehensive weight depends on the adjustment of the forward feedback mechanism, it is difficult to readjust the weight of the design index according to the standard evaluation results to establish a perfect feedback mechanism. In this paper, the optimization process is deeply integrated with power big data. The vast solution space defined by the comprehensive weights W is effectively navigated by the PSO algorithm thanks to the diversity of cases present in the big data. This diversity helps prevent overfitting and ensures the optimized weights are generalizable and robust. The convergence behavior of the PSO algorithm is improved because the big data provides a smoother and more informative fitness landscape, allowing the swarm to more efficiently locate the global optimum rather than becoming trapped in local solutions.

The particle swarm optimization algorithm was designed to optimize the objective function, as shown below:

$$Z = Y \times W \tag{29}$$

In the formula, Z represents a set of evaluation results generated, Y represents the random scoring matrix of each indicator, and W represents any set of comprehensive weights.

(1) Randomly initialize a group of particles, each particle represents a set of parameters (Y and W) of the electricity consumption prediction model, and randomly set the initial speed and position of each particle.

(2) Determine the individual historical optimal position and individual historical optimal fitness, and the group historical optimal position and group historical optimal fitness. Where, Z is used as the fitness function.

(3) In each iteration, the current fitness of each particle is compared with its historical best fitness, and the optimal position of the individual is updated. Update the speed and position of the particle based on the individual optimal and global optimal position, as well as the current velocity and position of the particle.

(4) Repeat the above steps (2 and 3) until a preset number of iterations is reached or other stopping conditions are met.

(5) After the iteration, select the parameters crresponding to the globally optimal particle as the parameters of the final prediction model.

(6) Use the optimized prediction model to calculate the prediction result Z.

5.4 *Carbon reduction synergy level in the power secto transition*

To verify the effectiveness of the weight optimization strategy proposed in this paper, the year 2050 will be taken as an example, and the following three distinct scenarios are established to assess and compare the synergy levels of carbon reduction resulting from the low-carbon transition of the power sector:

Scenario 1: Subjective weights of AHP;

Scenario 2: Objective weights of the EWM;

Scenario 3: Comprehensive weights of AHP-EWM-PSO.

Based on the scores and assigned weights of the carbon reduction evaluation indicators, the carbon reduction synergy level across the three scenarios ranges between 0.7 and 0.9. Scenario 3 yields the highest synergy level, attributable to the more scientific and rational comprehensive weighting achieved through the AHP-EWM-PSO algorithm. This elevated performance underscores the efficacy of the power sector's transition strategies, which include actively promoting clean energy sources—such as wind, solar, and hydropower—while reducing dependence on coal and other traditional energy sources. These measures significantly curtail carbon emissions and enhance the overall evaluation score. Furthermore, the adoption of clean energy not only reduces carbon emissions but also improves energy efficiency and power supply reliability. Additional efforts—such as optimizing energy consumption patterns, upgrading equipment efficiency, and strengthening energy management—contribute substantially to energy conservation and emission reduction, reinforcing the sector's progress toward a sustainable, low-carbon future.

5.5 *Carbon emission reduction and coordinated control outcomes*

Guided by projections of future power demand, this study emphasizes the optimization of the power supply structure as the central strategy for controlling total carbon emissions. As depicted in Figure 6, both carbon dioxide emissions and associated air pollutants demonstrate a consistent declining trend from 2030 to 2050, resulting from the systematic low-carbon transition of the power sector.

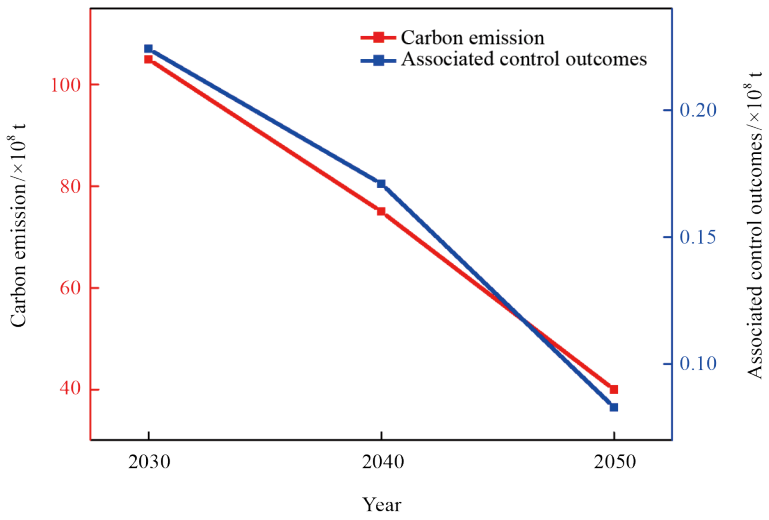

Figure 6. Total carbon dioxide and air pollutants

In 2030, total carbon emissions reached 10.3 billion tons, while air pollutants amounted to 22 million tons. By 2050, these values will decline significantly to 4.5 billion tons and 0.08 million tons, respectively. This marked reduction can be attributed to the strengthened policies phasing out coal-fired power and the large-scale integration of renewable energy sources, all implemented without compromising the growing demand for electricity. The low-carbon transformation of the power sector not only achieves substantial carbon emission reductions but also generates significant co-benefits, including the decline of air pollutants—a synergistic outcome reinforcing the environmental advantages of transitioning toward a clean energy system.

5.6 *Cooperation degree index of carbon reduction*

When ΔPM and ΔCM are less than zero, it indicates a successful reduction in carbon emissions, signifying that the power sector's low-carbon transition is effectively contributing toward emission mitigation targets. Under this structural transformation, the deployment of clean energy and phase-out of fossil-based generation also bring about a concurrent decrease in air pollutants, reflecting the inherent co-benefits of decarbonization. Observations from 2030 to 2050 confirm that both carbon emissions and atmospheric pollutants show a consistent declining trend.

5.7 *Synergistic coupling degree of carbon reduction*

Based on the carbon reduction synergy level (T) and the cooperation degree index (C), the comprehensive coupling coefficient TC approaches a value of 1. This indicates a high degree of coordination between the achieved carbon mitigation outcomes and the pathway of the power sector's transition, demonstrating that the system has met the conditions for entering a stage of synergistic low-carbon development.

6. Conclusion

On the premise of meeting future electricity demand, this study constructed a multi-level evaluation index model for the low-carbon transition of the power sector using an analytic hierarchy process. By integrating evaluation dimensions and influence strategies across different levels, the impact of various pathways on carbon reduction was thoroughly analyzed, enriching both the data foundation and analytical perspectives for assessing decarbonization outcomes. An improved entropy weight method was applied to enhance the objectivity and monitoring capacity of the carbon reduction synergy evaluation.

Further, based on comprehensive weighting and combined with actual emission reduction results, a final evaluative outcome for carbon reduction was generated, improving the objectivity, accuracy, and practical relevance of the assessment. By controlling cumulative carbon emissions, optimizing the power supply structure, and expanding the capacity and generation share of renewable sources—such as wind, hydropower, and photovoltaics—significant carbon emission reductions were achieved. Total CO_2 emissions declined markedly over the period, and the associated reduction in air pollutants—resulting from the clean energy transition—further underscores the multiple benefits of decarbonization. A key finding is that the model leverages existing power big data sources not merely as input, but as a catalyst for model optimization. The data-driven approach allows for a more accurate calibration of the model parameters and a more effective optimization of the indicator weights, directly contributing to the enhanced performance of the AHP-EWM-PSO hybrid scenario. This enhances feasibility by transforming preexisting infrastructure investments into actionable insights for strategic planning. The study demonstrates the critical role of power big data in advancing beyond theoretical models to create a practical, optimized, and high-fidelity decision-support tool for the low-carbon transition.

Comprehensive multi-dimensional analysis and in-depth mining of carbon emission data allow for precise identification of key sectors and vulnerable links in the carbon reduction process, supporting targeted policy and investment decisions for achieving deep decarbonization in the power industry.

Acknowledgement

This work is supported by the State Grid Tianjin Electric Power Science Research Institute's project "Research and Application of Key Technologies for Deep Low-Carbon Integration of 'City, Enterprise, and Grid' Based on Electric Power Big Data" (Science and Technology Project 2025-22).

Ethics approved

This paper does not involve additional human experiments, therefore, ethical committee approval or consent is not required.

Data availability statement

The original contributions presented in the study are included in the article, further inquiries can be directed to the corresponding author.

Conflict of interest

The authors declare no competing financial interest.

References

[1] Xian BT, Xu YL, Chen W, Wang Y, Qiu L. Co-benefits of policies to reduce air pollution and carbon emissions in China. *Environmental Impact Assessment Review*. 2024; 104: 107301.

[2] Chen XL, Di QB, Liang CL. Coupling relationship and interactive response between pollution control & carbon emission reduction and high-quality economic development in China's urban agglomerations. *Environmental Science*. 2024; 45(11): 1-18.

[3] Wang M, Yang RP, Li LP. Evaluation method and empirical study on synergistic reduction of pollution and carbon emissions at the urban level. *Progress in Climate Change Research*. 2024; 20(2): 242-252.

[4] Wang K, He Y. Study on the synergistic emission reduction effect between carbon dioxide and atmospheric pollutants on ultra-low emission retrofits of thermal power plants in Yunnan Province. *Journal of Environmental Science*. 2022; 41(2): 30-33.

[5] Liu K, Ren GX, Dong SM, Xue YT. The synergy between pollution reduction and carbon reduction in Chinese cities and its influencing factors. *Sustainable Cities and Society*. 2024; 106: 105348.

[6] Zha QF, Liu Z, Wang J. Spatial pattern and driving factors of synergistic governance efficiency in pollution reduction and carbon reduction in Chinese cities. *Ecological Indicators*. 2023; 156: 111198.

[7] Zhu FH, Xu JX, Pan C. Development situation and target prospect on the reduction of pollutant and carbon emissions in power industry. *Environmental Protection*. 2022; 50(10): 15-20.

[8] Xiang MY, Wang S, Lu LH, Zhang N, Bai ZH. Synergistic paths of reduced pollution and carbon emissions based on different power demands in China. *Environmental Science*. 2023; 44(7): 3637-3648.

[9] Liu MH, Yue YY, Liu SN, Li J, Liu JH. Multi-dimensional analysis of the synergistic effect of pollution reduction and carbon reduction in Tianjin based on the STIRPAT model. *Environmental Science*. 2023; 44(3): 1277-1286.

[10] Samane G, Dehghan SZ, Hossein A. Social, economic, and technical factors affecting CO_2 emissions in Iran. *Environmental Science and Pollution Research*. 2023; 30: 70397-70420.

[11] Urszula G, Roman A, Joanna N, Salahodjaev R. Renewable energy, urbanization, and CO_2 emissions: a global test. *Energies*. 2022; 15(9): 3390.

[12] Andrew JP, Jan P, Barbour ER, Cockerill TT. Using electricity storage to reduce greenhouse gas emissions. *Applied Energy*. 2021; 282: 116199.
[13] Stela D, Andrei CP. Experimental study on the determination of average concentrations of polluting emissions for a thermoelectric power plant. *MATEC Web of Conferences*. 2021; 342: 06005.
[14] Marion L, Philippe Q. Air pollution and CO_2 from daily mobility: who emits and why? Evidence from Paris. *Energy Economics*. 2022; 109: 105941.
[15] Zou XY, Mao XL. Research on the impact of carbon emissions trading market on corporate carbon reduction efforts in China. *Journal of Chongqing Normal University (Social Science Edition)*. 2023; 44(2): 70-82.
[16] Celil A, Yagmur C. Does the level of renewable energy matter in the effect of economic growth on environmental pollution? New evidence from PSTR analysis. *Environmental Science and Pollution Research International*. 2022; 29(54): 81624-81635.
[17] Salim R, Rafiq S, Shafiei S, Yao Y. Does urbanization increase pollutant emissions and energy intensity? Evidence from some Asian developing economies. *Applied Economics*. 2019; 51(36): 4008-4024.
[18] Saint SA, Adewale AA, Victor FB, Etokakpan MU. Does electricity consumption and globalization increase pollutant emissions? Implications for environmental sustainability target for China. *Environmental Science and Pollution Research International*. 2020; 27(20): 25450-25460.
[19] Fu XY, Zheng L. Optimal scheduling algorithm of renewable energy power generation considering security risk cost. *Acta Energiae Solaris Sinica*. 2025; 1-9. Available from: https://doi.org/10.19912/j.0254-0096.tynxb.2025-0487.
[20] Liao CH, Li G. Optimal allocation of wind-photovoltaic-battery storage capacity of multi-energy complementary energy base based on existing thermal power capacity. *Water Power*. 2024; 50(9): 74-81.
[21] Yuan JL, Jia XC, Fang D, Dong JF. Joint stochastic optimal scheduling of heat and power considering source and load sides of virtual power plant. *Power System Technology*. 2020; 44(8): 2932-2940.
[22] Yao YX, Ye L, Qu XX, Wang WS, Li P, Dong L. Exergy analysis model of wind-solar-hydro multi-energy generation power system. *Electric Power Automation Equipment*. 2019; 39(10): 55-60.
[23] Ara A, Zohora TF, Nurul N, Tanvir A, Ahmed N. Optimal site selection for solar plant using analytical hierarchy process (AHP): a case study in Bangladesh. *Environmental Progress & Sustainable Energy*. 2023; 43(2): e14272.
[24] Alimujiang A, Jiang P, Dong HJ, Hu B. Synergy and co-benefits of reducing CO_2 and air pollutant emissions by promoting new energy vehicles: a case of Shanghai. *Acta Scientiae Circumstantiae*. 2020; 40(5): 1873-1883.
[25] Sedighizadeh D, Masehian E, Sedighizadeh M, Akbaripour H. GEPSO: a new generalized particle swarm optimization algorithm. *Mathematics and Computers in Simulation*. 2021; 179: 194-212.
[26] Fei WL, Li YJ, Yang M, Tang YD, Zhang XL. Analysis of the synergistic path to reduce pollution and carbon in industrial parks under carbon peak and carbon neutrality targets. *Environmental Protection*. 2021; 49(8): 61-63.
[27] Pan YQ, Qi B, Li B. Research on zero carbon evaluation index system for new energy parks. *Inner Mongolia Electric Power*. 2023; 41(5): 12-18.
[28] Qian HQ, Xu SD, Cao J, Ren FZ, Wei WD, Meng J, et al. Air pollution reduction and climate co-benefits in China's industries. *Nature Sustainability*. 2021; 4(5): 417-425.
[29] Wu YJ, Liu YS, Yin L, Wang S, Zhang JC. Low carbon assessment on railroad tunnel project construction process by the grey clustering method. *Journal of Xi'an University of Technology*. 2023; 39(3): 353-359.
[30] Shao JJ. Research on weight optimization model based on rough set and particle swarm optimization. *Economic Research Guide*. 2022; 13: 43-47.
[31] Borni A, Bessous N, Zaghba L, Bouchakour A, Agmas MS, Ali E, et al. Enhancing grid connected wind energy conversion systems through fuzzy logic control optimization with PSO and GA techniques. *Scientific Reports*. 2025; 15(1): 27678.
[32] Xue J, Yang H, Song Y, Zhang C, Hu H. A fuzzy decision-making network model for offshore wind turbine selection based on simulated annealing algorithm. *Ocean Engineering*. 2025; 315: 119816.
[33] Godha DN, Dagade R, Bapat V, Korachagaon I. Polydomous ant colony optimization for distributed generation and capacitors placement in the context of techno-economic and environmental objectives. *Iranian Journal of Science and Technology, Transactions of Electrical Engineering*. 2025; 49: 2125-2143.
[34] Wang YN, Li BX, Zhang YX, Zhao Y, Miao CK, An JQ. Spatiotemporal characteristics and influencing factors of the synergistic effect of pollution reduction and carbon reduction in China. *Environmental Science*. 2024; 45(9): 4993-5002.

[35] Zhao SY, Xin C, Chen H, Jiang X, Yu ZB, Wang S, et al. Low-carbon evaluation system and solution optimization of transmission and transformation project based on AHP-EWM. *Guangdong Electric Power*. 2024; 37(1): 8-17.

[36] Yi L, Yang TT, Du X, Yang L, Deng W. Collaborative pathways of pollution reduction and carbon abatement: typical countries' driving mechanisms and their implications for China. *China's Population, Resources and Environment*. 2022; 32(9): 53-65.

Appendix

Table 5. Evaluation index of pollution and carbon reduction

Target layer	Criteria layer	Indicator layer
Synergistic evaluation of pollution and carbon reduction	Energy sector	Fossil energy share
		Percentage of new energy
		Contractual energy management penetration rate
		Wastewater discharge per unit of industrial added value
		Solid waste generation per unit of industrial added value
	Industrial sector	Emission elasticity coefficients for major pollutants
		Percentage of fuel vehicles
	Transportation sector	Percentage of new energy vehicles
		The ratio of public charging posts to electric vehicles
		Carbon dioxide emission
	Carbon Reduction Effect	Lower carbon dioxide emissions
		Carbon emission elasticity coefficient
	Ecology sector	Ecological quality index
		Green coverage
		Ecosystem stability
	Environment sector	Air quality
		Quality of the water environment
	Construction sector	Carbon productivity
		Coal-fired heating
		New energy heating
		Energy activities in construction
	Economy sector	Energy productivity
		Emerging industries as a percentage of GDP
		R & D investment intensity
	Institutional sector	Environmental subcontrol
		Well-established mechanism
		Completion of the smart platform